CBC 493/CM4073

NANYANG TECHNOLOGICAL UNIVERSITY

DIVISION OF CHEMISTRY AND BIOLOGICAL CHEMISTRY
SCHOOL OF PHYSICAL & MATHEMATICAL SCIENCES

Title: Design and synthesis of pH-responsive supramolecular vesicles based on rhodamine B derivative for anti-cancer drug delivery

Submitted by: Liu Yang

U1140952C

Supervisor: Asst. Prof. Zhao Yanli

Academic Year: 2014/2015 Semester 1

Contents

1 Acknowledgement

I would like to express my sincere gratitude to my supervisor Asst. Prof. Zhao Yanli for providing me the opportunity to conduct this research project, as well as for his invaluable guidance and kind encouragement throughout the project.

I would also like to thank my mentor Xu Xingdong for his great effort contributed to educate me on the subject of investigation, as well as his support, motivation and inspiring suggestions throughout the project.

I would also like to gratefully acknowledge Dr. Shi Huifang and Dr. Wang Jingui for their assistance in performing the transmission electron microscopy experiments, and to thank my seniors Chen Hongzhong and Feng Tao for their kindness and assistance during the last three months.

2 Abstract

A pH-responsive supramolecular vesicle based on an amphiphilic rhodamine derivative has been synthesized and characterized for potential application in controlled anti-cancer drug delivery. The mechanism for the targeted drug release is based on the hydrophobicity change of rhodamine moieties in acidic condition. The rhodamine-derivative forms stable vesicles in aqueous solution at normal physiological pH, while exhibit pH-sensitivity in the range of pH 5 to 7, which corresponds with the extracellular pH of tumor cells. The results suggest that rhodamine-based vesicles have great potential as pH-responsive nanocarriers for anti-cancer drug delivery and as imaging agents for acidic organelles.

3 Introduction

Since its discovery in mid 1960s, vesicular drug delivery systems have breathed new life into the existing anti-cancer formulations by dramatically increasing their bioavailability and reducing toxicity.[1] Following the successful implementation of liposome-encapsulated drugs such as Doxil and Lipodox, polymer-based vesicles have emerged as a promising candidate for next-generation nanocarriers due to their customizability, stability and potential for mass-production.[2] Recent research is not only focused on proposition of readily-synthesized vesicular building blocks, but also directed increasingly at targeted drug delivery triggered by physical or chemical stimuli present in the malignant tissue.[3]

One major difference between many solid tumors and healthy tissues is the acidic environment surrounding tumor cells. The pH value of extracellular fluid (pH_e) of solid-tumors is found to have a mean value of 7.0 with a full range of 5.7-7.8, while the pH_e of normal tissues falls around pH 7.2.[4] This phenomenon enables the development of pH-sensitive nanocarriers that allows triggered drug release at the tumor pH_e.

Rhodamine B is a fluorescent dye widely used in biology with relatively low toxicity.[5] Its derivatives containing a spiralactam moiety are well known for protonation-driven

ring-opening in acidic conditions.[6] Thus, a supramolecular vesicle constructed with amphiphilic rhodamine conjugates would disintegrate at low pH due to the decreased hydrophobicity of the protonated rhodamine moiety (Scheme 2). By changing the hydrophile, the range of pH-sensitivity can be altered to accommodate the pH range in tumor cells, thereby facilitating targeted drug release. However, despite various attempts, currently existing rhodamine-based vesicles are rarely of practical use in drug delivery due to difficulties in achieving the desired pH sensitivity and self-assembly patterns.

To contribute new insights into this field, we herein propose a novel rhodamine-based amphiphilic molecule, **RB-HP**, prepared by coupling reaction between a rhodamine B-diamine conjugate and a hydrophilic tri-substituted benzoic acid (Scheme 1). The molecule is capable of vesicle formation in aqueous solution, and exhibit significant pH-responsiveness in the range of tumor pH_e. Scheme 2 depicts the mechanism of disassembly of **RB-HP** vesicles in acidic conditions.

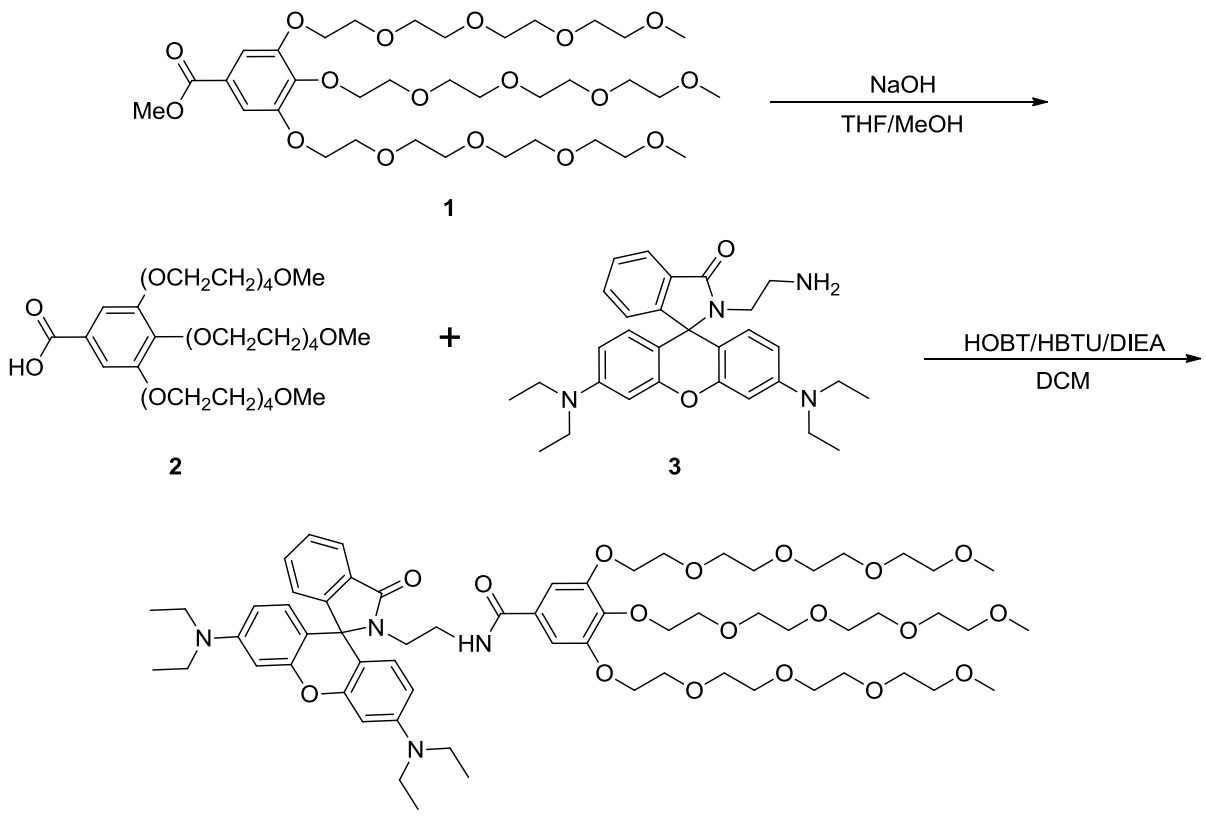

Scheme.1 synthesis of **RB-HP**

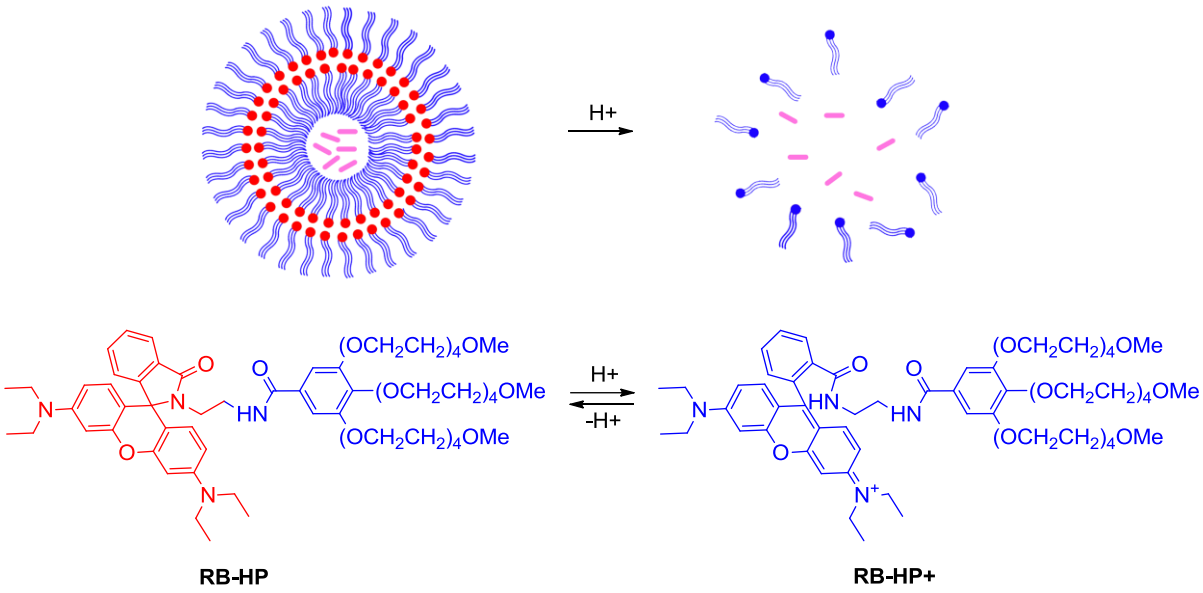

Scheme.2 drug release mechanism of **RB-HP** vesicles in acidic conditions

RB-HP in its neutral form is colorless and non-fluorescent, while addition of H^+ yields a conjugated ring system and fluorescence. Therefore, the pH response range of such molecule was conveniently determined by measurement of UV-Vis absorption and fluorescence emission. Meanwhile, measurement of UV-Vis transmittance and transmission electron microscopy (TEM) were also carried out to study the self-aggregation behavior of this amphiphile. It is found that **RB-HP** vesicles are stable in neutral conditions, while the individual molecules exhibit strong pH sensitivity in the range of pH_e of tumor cells. The results suggest potential application of RB-HP vesicles in anti-cancer drug delivery and imaging of acidic organelles.

Results and Discussion

RB-HP was readily synthesized from **2** and **3** with the addition of coupling agents. The vesicle-forming ability of the compound was first investigated through spectrophotometric determination of its critical micelle concentration (CMC). TEM was also carried out in order to identify the size and morphology of the aggregated structure. Furthermore, optical responses to pH were measured in dilute solution, from which pKa of the protonated **RB-HP**$^+$ (Scheme 2) was calculated, which provides an insight to the pH trigger point and sensitivity of the proposed nanocarrier.

3.1 Measurement of CMC

Figure 1 shows the transmittance of **RB-HP** solution with different concentration (0.3 mM – 1.5 mM). The transmittance changes at 450nm with respect to concentration were plotted in Figure 2.

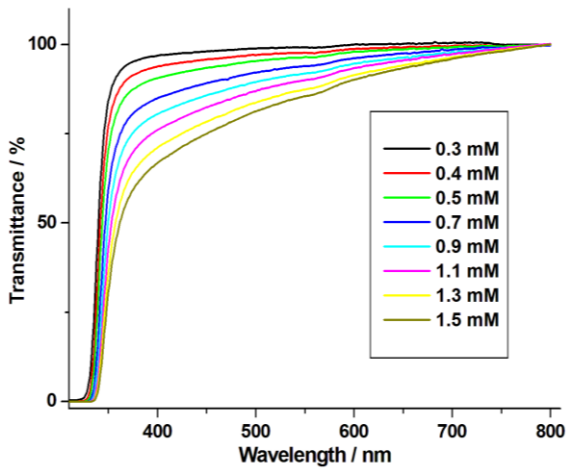

Fig. 1 transmittance spectra of **RB-HP** in 20 mM AcOH/NaAc buffer solution (pH = 7.0) with different concentration

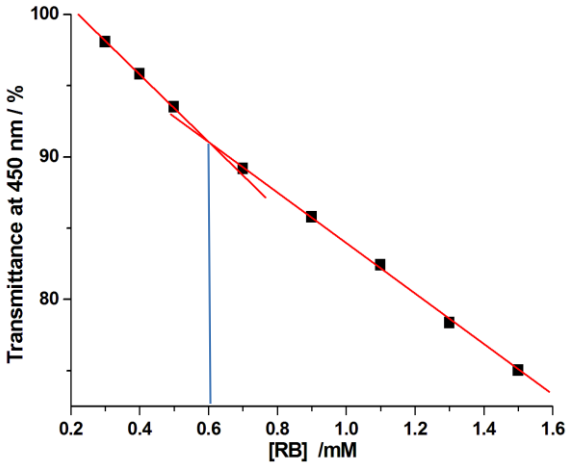

Fig. 2 the transmittance changes at 450 nm with respect to [**RB-HP**]

The transmittance of the solutions, which is relevant to the concentration and solvation state of the solute, decreases gradually as concentration increases, with an inflection point at [RB-HP] = 0.6 mM. The inflection point in the curve is indicative of the onset of

agglomeration within the solution and is therefore a good estimation of the critical micelle concentration.[7]

3.2 TEM Imaging of vesicles

The TEM sample was prepared by evaporation of a droplet of 0.5mM **RB-HP** solution. Multiple images of microstructures present within the solution were obtained (Figure 3).

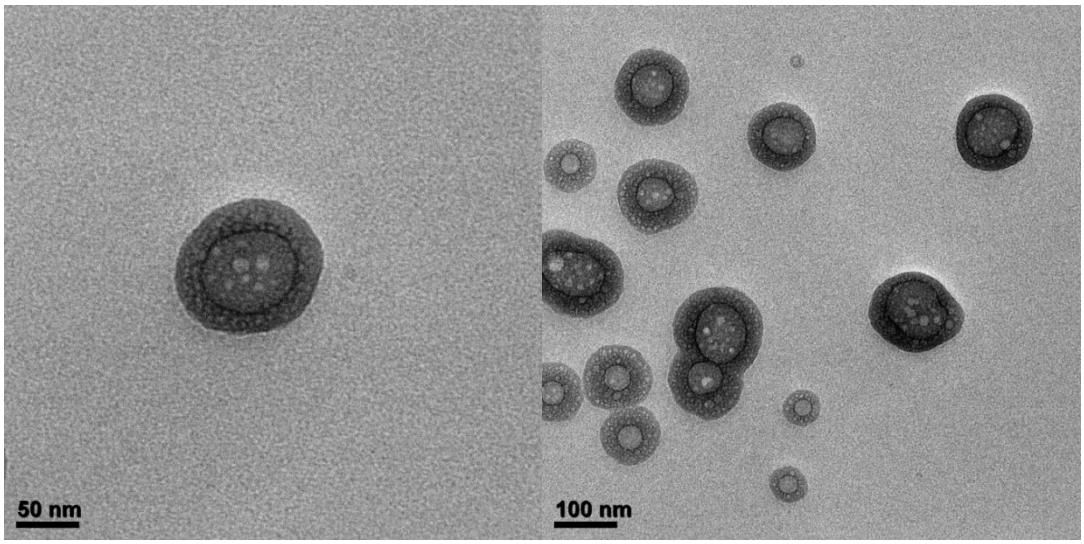

Fig. 3 TEM images of a dried droplet of 0.5mM **RB-HP** solution

The pictures show spherical morphology of ca. 100nm diameter with a unilamellar structure. The mean membrane thickness is measured to be ca. 25 nm. While the drying process during sample preparation may induce deformation of native morphology,[8] the images provide valuable proof of the existence of vesicles and estimation of their membrane thickness, which is less prone to change during the drying step.

3.3 Optical responses to pH

The UV-Vis absorption spectra of RB-HP (10 μM) in 20 mM buffer solution with different pH, together with the plot of absorbance vs. pH at 580 nm, are presented in Figure 4 and 5. The fluorescence emission spectra and the corresponding plot at 580 nm are subsequently shown in Figure 6 and 7.

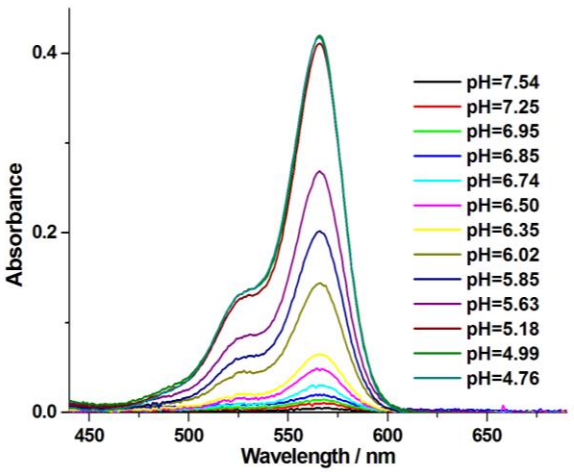

Fig. 4 absorption spectra of 10 μM **RB-HP** in 0.2 M AcOH/NaAc buffer solution with different pH

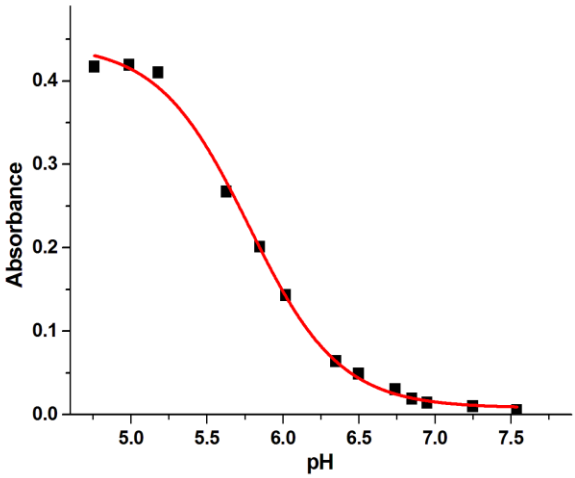

Fig. 5 absorbance changes at 580 nm with respect to pH

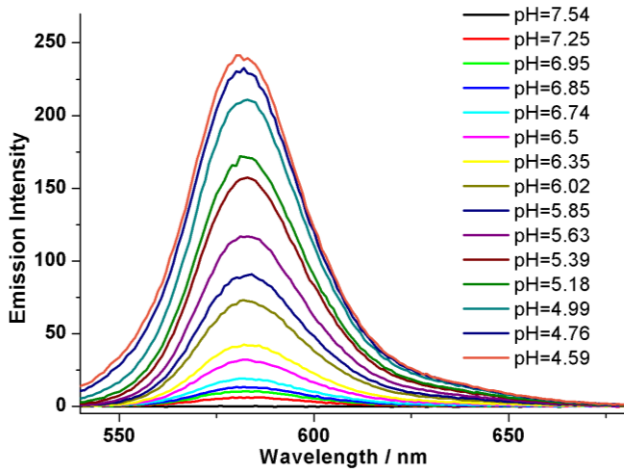

Fig. 6 fluorescence emission spectra of 10 μM **RB-HP** in 0.2 M AcOH/NaAc buffer solution with different pH

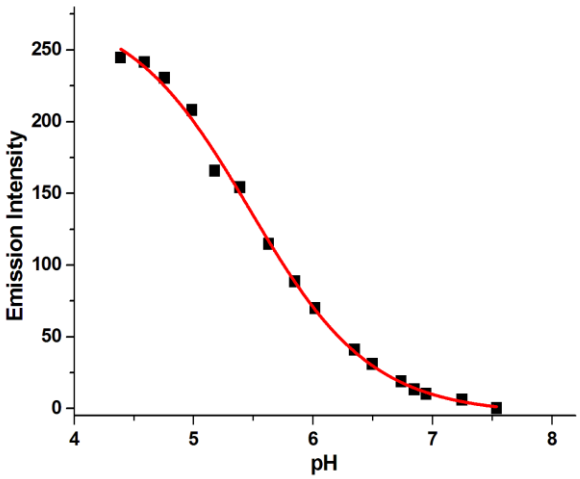

Fig. 7 emission changes at 580 nm with respect to pH

The fit curves in Figure 5 and 7 resemble the shape of a titration curve, where absorbance/emission intensity falls with decreasing [H^+]. The shape evidently arises from deprotonation of the fluorescent rhodamine moiety in RB-HP^+, which gives the non-fluorescent RB-HP, leading to fluorescence quenching (Scheme 2). The absorbance/emission intensity changes by 20 folds within the pH range of 5 to 7, indicating a very good sensitivity comparable to many commercial pH probes suitable for biological applications.

Based on Figure 5 and 7, a linear fit according to Henderson-Hasselbach equation yields pKa = 5.77(4)*, with an active range from pH 5.0 to pH 7.0 where the concentration of the protonated form changes drastically. The pH response covers the range of extracellular pH of tumor cells (5.7 - 7.8), while being relatively insensitive in the pH range of normal tissue and muscle (7.0 - 8.1).[4] It suggests the great potential of **RB-HP** vesicles as an anti-cancer drug carrier, whose disintegration can be triggered by the acidic extracellular or early endosomal pH of malignant cells. Moreover, the compound reaches full protonation at about pH 5, which coincides with the lysosomal pH,[9] suggesting its potential application as imaging agents or building blocks for intracellular drug carriers targeting acidic organelles.

It is worth noting that the above measurement was conducted in dilute solution with the sample concentration significantly less than the critical micelle concentration. Thus the behaviors observed were of single solvated molecules, which serve as an indicator of the pH responsiveness of the corresponding supramolecular vesicles. Further investigation is required to accurately describe the pH response of **RB-HP** vesicles and its release pattern in cancer cells.

4 Conclusion

A novel supramolecular vesicle based on a rhodamine derivative has been synthesized and its pH responsiveness studied with fluorescence and UV-Vis spectroscopy. The dye constructing the vesicles gradually ionizes and show fluorescence at around pH = 5.77, while being neutral at normal physiological pH. It can be inferred that the vesicles would disintegrate as the dye is ionized and loses its amphiphilicity, suggesting its potential application in targeted drug delivery to acidic extracellular environment of tumor cells. The ease of synthesis, desirable pH sensitivity range and fluorescence properties of such vesicles make them a very promising agent for anti-cancer drug delivery and cell imaging.

5 Experimental

5.1 Materials

The tri-substituted phenyl ester, **1**, and the rhodamine-diamine conjugate , **3**, are prepared according to literature methods.[10]

*5.2 Synthesis of **2***

1 (1.62 g, 2.15 mmol) was dissolved in a mixture of THF (20 ml) and MeOH (20 ml). Excessive amount of NaOH (0.86g, 21.5 mmol) was added to the solution and refluxed for 2 h. The solvent was then removed in vacuum. The precipitate was redissolved in DCM, neutralized with HCl, washed with water (20 ml × 2) and dried with Na_2SO_4. The resultant was concentrated in vacuum to give a colorless oil (1.41 g, 89%). ^{1}H NMR δ 7.42 (s, 2 H), 4.25-4.22 (comp, 6 H), 3.84-3.69 (comp, 6 H), 3.70-3.53 (comp, 36 H), 3.41 (s, 6 H), 3.38 (s, 3 H).

*5.3 Synthesis of **RB-HP***

2 (540 mg, 0.729 mmol) was dissolved in DCM (20 ml). Excessive amount of 3 (443 mg, 0.911 mmol), HOBT (123 mg, 0.911 mmol), HBTU (345 mg, 0.911 mmol) and DIEA (235 mg, 1.82 mmol) were added and the solution was stirred at room temperature for 12 h. The solvent was then removed in vacuum. The precipitate was redissolved in DCM, washed with water (20 ml × 2), dried with Na_2SO_4 and concentrated in vacuum. The resultant was purified by column chromatography (silica gel, first: DCM/MeOH = 9:0.5, v/v, second: acetone/hexane = 3:2, v/v) to afford a light-yellow oil (600 mg, 68%). ^{1}H NMR (300MHz, $CDCl_3$) δ 8.36 (br, 1 H, NH), 7.89-7.86 (m, 1 H), 7.49-7.47 (comp, 2 H), 7.23 (s, 2 H), 7.12-7.10 (m, 1 H), 6.47-6.41 (comp, 4 H), 6.29 (dd, *J* = 8.9 Hz, 2.6 Hz, 2 H), 4.32 (t, *J* = 5.2 Hz, 4 H), 4.22 (t, *J* = 5.6 Hz, 2 H), 3.95 (t, *J* = 4.7 Hz, 4 H), 3.83 (t, *J* = 5.2 Hz, 2 H), 3.80-3.78 (m, 4 H), 3.76-3.74 (m, 2 H), 3.72-3.66 (comp, 20 H); 3.58-3.55 (comp, 6 H), 3.47-3.45 (m, 5 H), 3.40-3.35 (comp, 13 H), 3.15-3.12 (m, 2 H), 1.19 (t, *J* = 7.0 Hz, 12 H); ^{13}C NMR (100MHz, $CDCl_3$) δ 170.48, 166.48, 153.28, 152.33, 148.98, 128.35, 123.93,

108.34, 106.31, 104.49, 97.75, 77.32, 77.00, 76.68, 72.34, 71.92, 70.78, 70.68, 70.61, 70.58, 70.49, 69.68, 68.64, 66.03, 59.00, 44.34, 12.59, -0.03; MS: anal. calcd for $C_{64}H_{94}N_4O_{18}$: 1206.7; found: 1224.0 ($M+H_2O$, 100%).

5.4 Analysis

Fluorescence spectra were acquired on a Shimadzu RF-5301PC fluorescence spectrometer. UV-Vis spectra were acquired on a Shimadzu UV-3600 spectrometer. Both measurements were carried out with 1-cm quartz cells. The sample solutions were prepared using 0.2 M AcOH/NaAc buffer and left to stabilize for 8 hours at room temperature (293 K). Each sample was shook thoroughly prior to the measurements to prevent sedimentation.

TEM was done with a JEOL JEM 1400 electron microscope. The sample was prepared as a micro droplet on a copper mesh with diameter of 3 mm and was allowed to evaporate overnight. ^{1}H NMR spectra were acquired on a Bruker AV 300 spectrometer, and ^{13}C NMR spectra on a Bruker AV 400 BBFO1 spectrometer at room temperature in $CDCl_3$. MS spectra were obtained on a ThermoFinnigan PolarisQ mass spectrometer with acetone as the solvent.

6 References

1. Kamboj, S.; Saini, V.; Maggon, N.; Bala, S.; Jhawat, V., *International Journal of Drug Delivery; Vol 5, No 2 (2013): International Journal of Drug Delivery* **2013**.
2. Shinde, N. G.; Aloorkar, N. H.; Kulkarni, A. S., *Research Journal of Pharmaceutical Dosage Forms and Technology* **2014,** *6* (2), 110-120.
3. Duan, Q.; Cao, Y.; Li, Y.; Hu, X.; Xiao, T.; Lin, C.; Pan, Y.; Wang, L., *J. Am. Chem. Soc.* **2013,** *135* (28), 10542-10549.
4. Amiji, M. M., *Nanotechnology for Cancer Therapy*. Taylor & Francis: 2006.
5. Marking, L. L., *The Progressive Fish-Culturist* **1969,** *31* (3), 139-142.
6. Zhang, W.; Tang, B.; Liu, X.; Liu, Y.; Xu, K.; Ma, J.; Tong, L.; Yang, G., *The Analyst* **2009,** *134* (2), 367-71.
7. Cai, L.; Gochin, M.; Liu, K., *Chem. Commun.* **2011,** *47* (19), 5527-5529.
8. Méndez-Vilas, A., *Current Microscopy Contributions to Advances in Science and Technology*. Formatex Research Center: 2012.
9. Cooper, G. M., *The Cell - A Molecular Approach 2nd Edition*. Sunderland (MA): Sinauer Associates: 2000.
10. Dujols, V.; Ford, F.; Czarnik, A. W., *J. Am. Chem. Soc.* **1997,** *119* (31), 7386-7387.

7 Appendix

Appendix I. Determination of pKa.

This method for determination of pKa is commonly used in laboratories for its practicability, good sensitivity and high throughput. The theoretical foundation is that absorption/emission intensity of a given compound in solution is directly proportional to its concentration when all other factors are kept constant, i.e.,

$$\mathrm{A\ (F)\ =\ kC}$$

where k is a constant. Therefore, the concentration terms in Henderson–Hasselbalch equation can be substituted by A (or F), giving the following equation:

$$\mathrm{pH = pKa + \log_{10}\frac{[A^-]}{[HA]} = pKa + \log_{10}\frac{\frac{A_i}{k}-\frac{A}{k}}{\frac{A}{k}} = pKa + \log_{10}\frac{A_i - A}{A}}$$

assuming that [HA] is the fluorescent species. A_i is the maximum absorbance when all sample molecules are in the protonated form, which in our case is the absorbance at around pH 3. The fluorescence intensity follows exactly the same equation.

A linear fit to the scatter plot of pH vs. absorbance gives pKa as the slope of the regression line. The data sheet and plots are presented below.

Table A1 data sheet for pKa calculation

pH	A	F	$\log_{10}[(A_i\text{-}A)/A]$	$\log_{10}[(F_i\text{-}F)/F]$
7.25	5.897	-	1.60716	-
6.95	9.997	0.014	1.3704	1.45918
6.85	13.148	0.019	1.24553	1.32113
6.74	18.693	0.03	1.08218	1.11059
6.5	30.867	0.049	0.8403	0.87565
6.35	40.937	0.064	0.69672	0.74159
6.02	69.949	0.143	0.3973	0.28241
5.85	88.367	0.201	0.24738	0.03126

5.63	114.622	0.267	0.05448	-0.25042
5.39	153.953	-	-0.23021	-
5.18	165.6	-	-0.32163	-
4.99	207.86	-	-0.75306	-
4.76	230.39	-	-1.21097	-
4.59	241.395	-	-1.88181	-

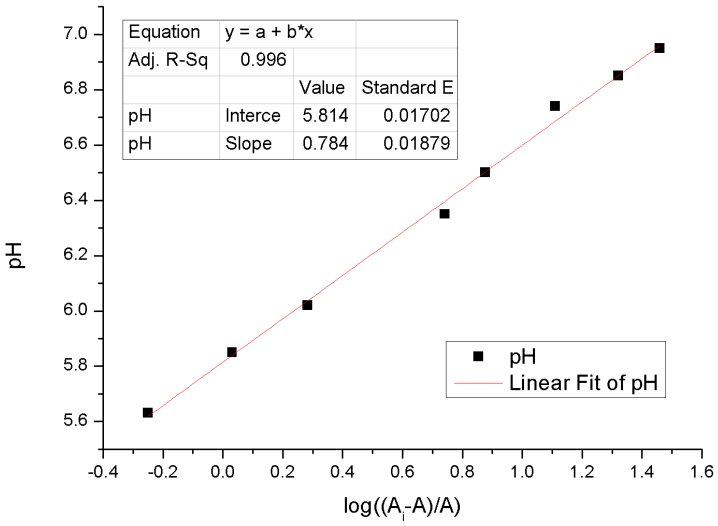

Fig. A1 scatter plot and linear fit of pH vs. $\log_{10}[(A_i-A)/A]$

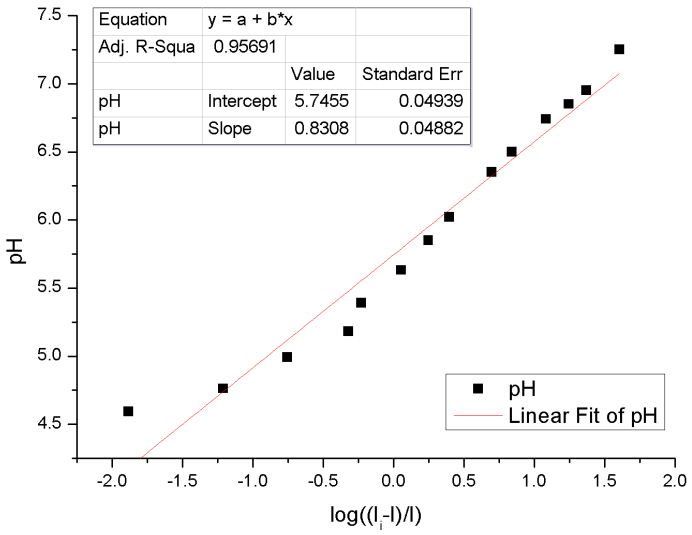

Fig. A2 scatter plot and linear fit of pH vs. $\log_{10}[(F_i-F)/F]$

The linear regression gives pKa = 5.81(2) and pKa = 5.74(5) for absorption and fluorescence measurements, respectively. The average value is 5.77(4).